energies

MDPI

Article

Design and Experimental Analysis of Multi-Functional Building-Integrated PV System for Adaptive Energy Generation and Thermal Management

Tahsin Boyekin [1,2,*], Tayfur Gökçek [3], Ali Rıfat Boynueğri [1,3] and İsmail Kıyak [4]

[1] Department of Electrical Engineering, Faculty of Electrical and Electronics, Yildiz Technical University, Davutpasa Street, Esenler, 34220 Istanbul, Türkiye; alirifat@yildiz.edu.tr
[2] Dal Solar Energy, Sirinevler, 34188 Istanbul, Türkiye
[3] BATLAB Research Center, Clean Energy Technologies Institute, Yildiz Technical University, Davutpasa Street, Esenler, 34220 Istanbul, Türkiye; gokcek.tayfur@gmail.com
[4] Department of Electrical and Electronics Engineering, Marmara University, Maltepe, 34854 Istanbul, Türkiye; imkiyak@marmara.edu.tr
* Correspondence: tahsinboyekin@gmail.com

Abstract

This paper introduces a hybrid building-integrated photovoltaic façade that brings together a 240 Wp mono PERC photovoltaic (PV) module and an electrically switchable Polymer Dispersed Liquid Crystal glazing unit within a single layered component. The main novelty of the proposed system is that the PV module and the smart glass layer are not treated as independent façade elements; instead, they are integrated to create a direct optical and functional interaction within the same building envelope component. The design enables controlled interaction between solar radiation, the PV cells, and the interior environment. By adjusting the optical state of the glazing, the façade can influence the amount of light entering the building while also affecting the irradiance received by the PV cells. In this way, the proposed façade provides two adaptive operating modes: a transparent mode that supports daylight transmission and indoor visual comfort, and a non-transparent mode that enhances effective irradiance on the PV cells through diffuse reflection. Experimental investigations carried out under real outdoor conditions, together with finite element thermal modeling, are used to evaluate electrical output and temperature behavior. Unlike conventional BIPV or smart glass applications, the proposed structure simultaneously addresses electricity generation, daylight regulation, and thermal management in a single multifunctional façade system. The results indicate that the integrated configuration yields nearly 4% higher energy production compared to a reference PV module, and that electrical output increases by about 5% when the glazing is in its non-transparent state. These findings highlight the potential of the proposed system to enhance both on-site electricity generation and indoor environmental performance in sustainable building applications.

Keywords: building-integrated photovoltaic; energy efficiency; polymer dispersed liquid crystal; smart glass thermal management

Check for updates

Academic Editor: Piero Bevilacqua

Received: 4 May 2026
Revised: 18 June 2026
Accepted: 4 July 2026
Published: 14 July 2026

Copyright: © 2026 by the authors. Licensee MDPI, Basel, Switzerland. This article is an open access article distributed under the terms and conditions of the Creative Commons Attribution (CC BY) license.

1. Introduction

1.1. Motivation and Background

A country's ability to meet its energy needs through its own resources is no longer viewed solely as an economic necessity, but also as a fundamental component of strategic

independence and national security. The continuous growth in global energy demand, the limited availability of fossil fuel reserves, and the adverse impacts of carbon emissions on climate change have made the transition toward renewable and low-carbon energy technologies unavoidable [1,2]. In this context, the effective utilization of sustainable energy resources has become critically important from both environmental and economic perspectives. Among renewable energy sources, solar energy stands out due to its high potential and its wide geographical availability. The fact that solar radiation reaches almost every region where life exists, either directly or indirectly, makes this energy source a scalable and practical option. These advantages have led to the rapid expansion of solar energy technologies; in particular, photovoltaic (PV) systems have gained prominence thanks to their technological maturity and their adaptability to various application areas [3].

In recent years, Building-Integrated PV (BIPV) systems, which enable the application of PV systems at the building scale, have been considered an important solution for sustainable energy generation, particularly in urban areas. These systems are generally designed to operate in connection with the grid. The building's energy demand is supplied by the grid when solar irradiation is insufficient, while the excess electricity generated is fed back into the grid when solar conditions are suitable. This bi-directional energy flow makes BIPV systems a flexible and effective structure in terms of both energy production and energy management [4,5]. User comfort, visual comfort, thermal performance, and indoor environmental quality in addition to energy generation have become increasingly important in modern building design [6]. In this context, technological developments in glass-based building components have drawn significant attention. Since the 1950s, advancements in glass and glass-based materials have enabled building envelopes to evolve from purely passive elements into active and functional components [7]. One of the most notable examples of these developments is the emergence of systems whose light transmittance can be adjusted through electrical stimulation, commonly referred to in the literature as smart glass or switchable glass [8]. Smart glass technologies are generally classified into two main groups as passive and active systems. Passive systems respond to environmental stimuli, while active smart glass can be electrically controlled and dynamically adjusted through user input or sensor-based systems. This controllability makes smart glass an important building component for improving indoor visual and thermal comfort [9].

On the other hand, Polymer Dispersed Liquid Crystal (PDLC) smart glass is an electrically switchable glazing material in which liquid crystal droplets are dispersed within a polymer matrix. In the absence of an electric field, the liquid crystal droplets are randomly oriented, causing incident light to be scattered and giving the glass an opaque appearance. When an electric field is applied, the droplets align with the field direction, allowing light to pass through the material and resulting in a transparent state. Therefore, the optical behavior of PDLC glass is mainly governed by the electrically controlled transition between light scattering and light transmission. In the proposed system, this property enables the façade to dynamically regulate indoor daylight while also influencing the amount of solar radiation reflected back toward the PV cells.

1.2. Literature Overview

Dias et al. [10] examined the use of building thermal mass to mitigate short-term BIPV output fluctuations caused by passing clouds. Cloud regimes were identified, and the impact of deactivating the cooling system was evaluated. The thermal mass acted as a low-cost storage, resulting in a 60% reduction in grid energy demand. Rajoria et al. [11] evaluated BIPV-integrated thermal systems using experimental data. It was found that system efficiency depended on design and climatic conditions. Water-based systems showed better performance than air-based ones, increasing electrical efficiency by up to 20% and

reducing thermal energy consumption by nearly 60%. Hendinata et al. [12] developed an integrated PV–electrochromic system to improve building energy management. A tungsten oxide layer was used within the electrochromic structure. It was reported that the combined system maintained optical performance while enabling significant transmittance variation, supporting both energy efficiency and dynamic light control. Saura et al. [13] presented a design for self-powered portable electrochromic devices. Scalable deposition methods and materials such as PEDOT-PSS, V_2O_5, and organic PV were investigated. A control strategy was implemented, and material optimization and scalability were examined. The applicability of the system to automotive glazing was also evaluated. Huang et al. [14] developed a PV–EC device with an electrochromic layer placed between transparent and semi-transparent substrates. Light-induced photopotential triggered redox reactions and color change. The system was observed to regain transparency under low light, while the generated energy was utilized within the device. Ma and Chen [15] proposed an integrated system combining BIPV and smart glass to optimize indoor lighting conditions. The smart glass was controlled based on the voltage generated by the PV module, maintaining a stable illumination level. However, the feasibility of the design depended on developing alternative materials due to the scarcity of indium. A PV-assisted electrochromic smart window system targeting net-zero energy buildings was developed in [16]. The system supplied the energy demand of the electrochromic layer through PV and enabled energy recovery. The results indicated an 18% reduction in building energy consumption and an annual saving potential of 318.4 MJ/m^2. The work [17] developed a modular smart window integrating PV and electrochromic technology. The transmittance of the window was dynamically controlled using the energy generated by the PV system. Improved indoor daylight uniformity and visual comfort were observed, while energy consumption was reduced by 10–15% compared to conventional systems. The paper [18] proposed a BIPV window system integrating crystalline silicon PV modules with electrochromic glass. Advanced control strategies were implemented, and solar radiation was reduced by more than 80%, leading to lower thermal loads. The results indicated that annual energy consumption could be reduced by over 60%. Wu et al. [19] developed a smart window system integrating PV and electrochromic glass. The energy generated by the PV module was directly used to control the glass, enabling dynamic adjustment of indoor lighting. Electrical generation and illumination performance were jointly evaluated under different conditions through experimental testing. A layered system integrating PV and electrochromic technologies was developed in [20]. PV, electrochromic, and transparent regions were separately designed to optimize performance. Simulation results indicated a useful daylight ratio of 79.88% and energy savings of approximately 13.7% under high irradiance conditions. The energy performance of semi-transparent PV and electrochromic glazing systems were compared in [21]. Experimental analyses showed a strong dependency on irradiance and temperature. It was also reported that existing testing standards were insufficient for accurately evaluating such systems. Naturally ventilated photovoltaic wall panels by considering air-cooled channel dimensions, temperature distribution, and airflow behavior were analyzed by Zheng et al. [22]. The study mainly focused on improving PV cooling performance through ventilation-channel design.

Based on the critical review summarized in Table 1, it is evident that studies integrating PV technology with smart glass are still limited and present several gaps. Existing applications mainly include smart glass systems with small embedded PV cells that generate electricity for their own consumption. Beyond this, vehicle and building glass applications have mostly been investigated at an experimental level. As shown in the table, a key limitation is the low efficiency of combined PV–smart glass systems, where the generated electricity is often only sufficient to meet the internal demand of the smart glass.

In addition, most studies lack detailed thermal modeling and analysis, while some rely solely on simulations. Overall, there is a clear need for a comprehensive, interdisciplinary approach that considers the system as a whole and aims to improve overall performance. In this study, the identified gaps in the literature are addressed by considering integrated system design, detailed thermal analysis, and both simulation and experimental validation, thereby improving overall efficiency and enabling a more comprehensive PV–smart glass application.

Table 1. Taxonomic table for the related literature works.

Reference	Thermal Management	Electricity Generation	Smart Glass	PV Module	PV Efficiency	Material Availability
[10]	✓	✓	✗	✓	High	✓
[11]	✓	✓	✗	✓	High	✓
[12]	✗	*	✓	✓	Low	✓
[13]	✗	*	✓	✓	Low	✓
[14]	✗	*	✓	✓	Low	✓
[15]	✗	*	✓	✓	Low	✓
[16]	✗	*	✓	✓	Medium	✓
[17]	✗	*	✓	✓	Medium	✓
[18]	✓	✓	✓	✓	Medium	✓
[19]	✗	*	✓	✓	Medium	✓
[20]	✗	*	✓	✓	Medium	✓
[21]	✓	✓	✓	✓	Medium	✓
This Paper	✓	✓	✓	✓	High	✓

(*) For only internal electricity demanded by the smart glass.

1.3. Contribution and Organization

In this study, a novel hybrid façade system is proposed in which a PV module and an electrically controllable Polymer Dispersed Liquid Crystal (PDLC) smart glass panel are integrated into a single building component. In the light of the BIPV works presented in the literature, the major contributions of the paper are as follows:

1. Unlike conventional approaches, the PV module and the smart glass are not only placed within the same building element, but also interact with each other optically in the proposed system. Through this approach, the system can operate in two distinct modes as an energy mode, in which the opaque state prioritizes electricity generation and helps maintain thermal balance, and as a comfort mode, in which the transparent state enhances daylight utilization and visual comfort.
2. Compared with previous PV–smart glazing and PV-electrochromic studies, the technical contribution of this study lies in the prototype-level integration of a high-power mono PERC PV module and a PDLC smart glass unit within a single façade component. The proposed structure enables the optical state of the PDLC layer to influence the effective irradiance received by the PV cells. In addition, the study combines outdoor electrical testing, module-level thermal monitoring, and ANSYS-based thermal validation to evaluate the electrical–thermal behavior of the integrated system.

The remaining parts of the paper is organized as follows: system description is presented in Section 2, simulation and experimental results are compared and discussed in Section 3, and finally, the conclusion of the study is evaluated in Section 4.

2. Preliminaries and Overview of the Proposed Structure

The developed integrated system has a multilayer architecture that combines PV generation with user-controlled light and thermal management within a single building component.

The proposed system consists of a multilayer structure including a 3.2 mm tempered outer glass, a 48-cell mono PERC PV panel with a total EVA thickness of approximately 0.6 mm and a rated power of 240 Wp, a 4 mm tempered inner glass, an air gap of about 2 mm, and an 11 mm laminated PDLC smart glass panel. The system is installed within an aluminum frame with internal dimensions of 1750 × 980 mm and is supported by a PDLC driver and control units, a Maximum Power Point Tracking (MPPT), and a grid-connected inverter. In addition, sensors and measurement devices that monitor ambient conditions enable continuous tracking of system performance and environmental parameters.

The detailed cross-sectional structure of the system is presented in Figure 1. This architecture is designed to enable optical and thermal interaction between the PV module and the PDLC layer. From the exterior to the interior, the structure consists of a laminated BIPV module, an air gap of approximately 2 mm, and a laminated PDLC smart glass panel, and it operates in two different modes. When the PDLC smart glass switches to the opaque mode, it behaves as a diffuse reflector and reflects a portion of the solar radiation that has passed through the PV module. This effect increases the effective irradiance reaching the rear surface of the PV cells and activates the photon recycling mechanism.

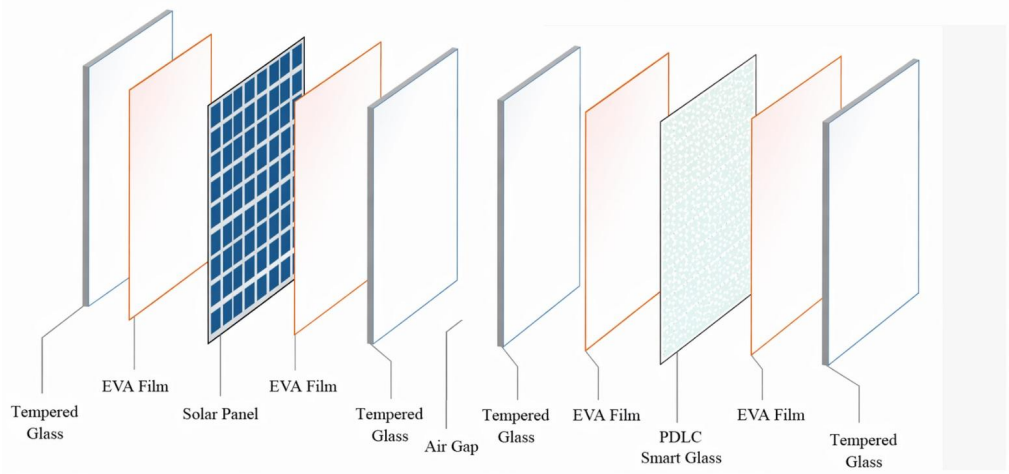


Figure 1. Cross-sectional structure of the system.

The PV module consists of 48 half-cut mono PERC cells, each rated at 5 Wp and measuring 210 × 105 mm, and the cells are electrically connected in series as demonstrated in Figure 2. Under standard test conditions (1000 W/m^2, AM 1.5, 25 °C), the module delivers a maximum power of 240 Wp, with an open-circuit voltage of 32.5 V, a short-circuit current of 9.11 A, a maximum power point voltage of 27.7 V, and a maximum power point current of 8.67 A. The cell layout geometry is presented in Figure 3, and the gaps between the cells account for approximately 38% of the total surface area.

As a result of integrating the PV module with the PDLC smart glass, the effective irradiance incident on the PV cells and the corresponding cell temperature are altered. In particular, when the PDLC operates in the opaque mode, a portion of the radiation transmitted through the PV module is diffusely reflected back, thereby increasing the effective irradiance received by the cells. The effect of the increase in cell temperature on electrical performance has been evaluated using (1) and (2) that describe the temperature-dependent changes in current and voltage, respectively. Based on these calculations, the electrical compatibility between the PV module and the inverter has been verified.

$$V_{oc}(t) = V_{oc} + \left(V_{oc} \times \left(\frac{k_{v_{oc}}}{100} \times (t - t_{st}) \right) \right) \quad (1)$$

$$I_{sc}(t) = I_{sc} + \left(I_{sc} \times \left(\frac{k_{i_{sc}}}{100} \times (t - t_{st}) \right) \right) \quad (2)$$

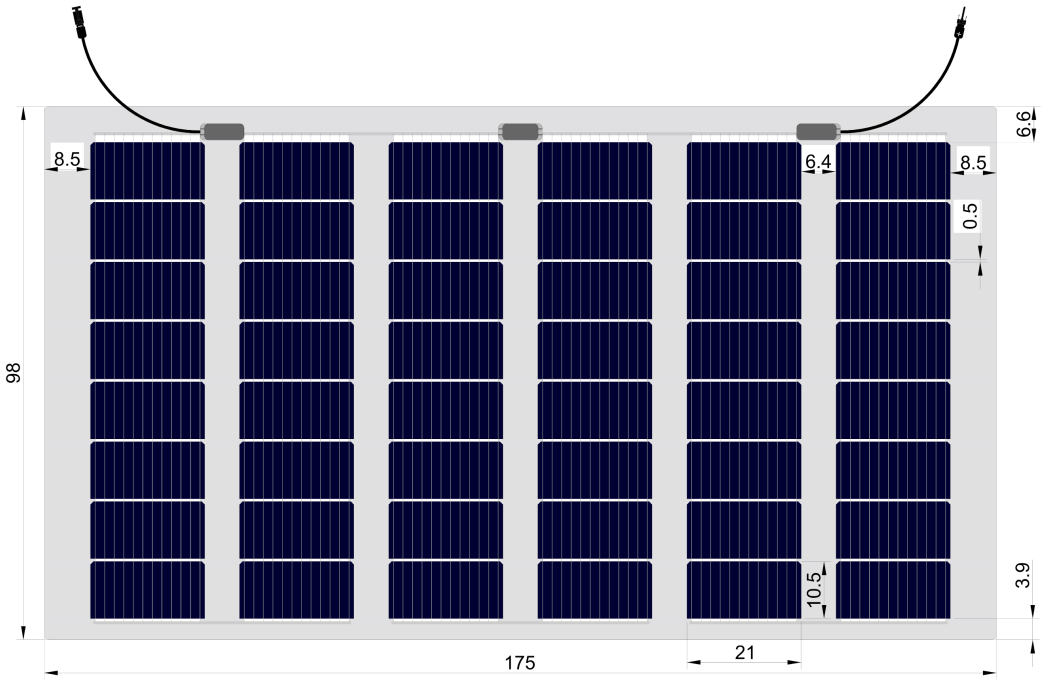


Figure 2. The cell layout geometry.

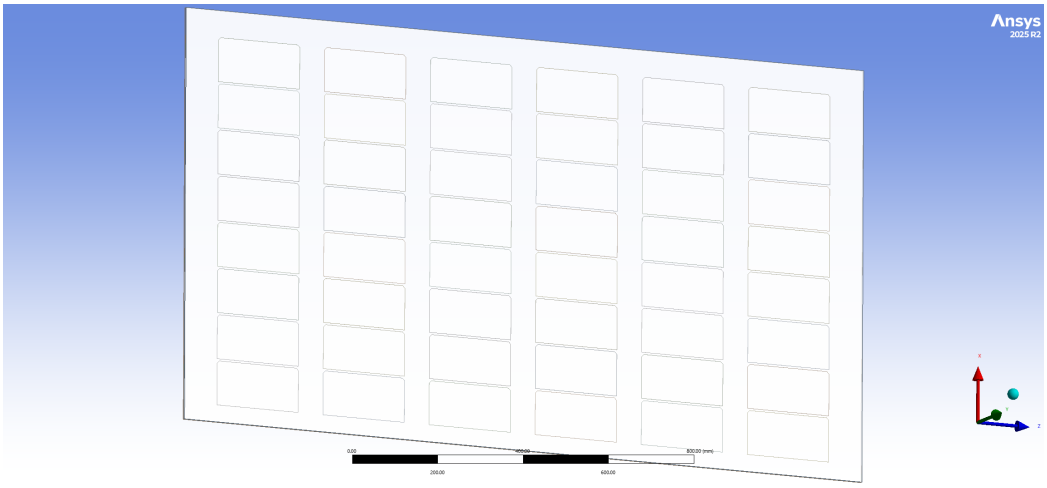


Figure 3. ANSYS-based model (2025 R2).

In the experimental studies, solar irradiance, current, voltage, power, and temperature parameters are measured simultaneously. The thermal behavior of the system is continuously monitored using an infrared thermal camera. Comprehensive thermal and electrical measurements are carried out to evaluate in detail the effects of irradiance intensity, current, voltage, and temperature. Current and voltage values are measured both at the output of the PV module and at the grid connection point. During the measurements, solar irradiance and ambient temperature are recorded simultaneously, while the thermal response of the system is continuously observed through thermal imaging. The tests aim to reveal the impact of smart glass integration on the electrical output of the PV module as well as the resulting change in thermal load on the module. In this context, the proposed PV–smart glass module is manufactured in accordance with the defined architecture and tested under real solar radiation at different irradiance levels. The system response under varying

irradiance conditions is analyzed, and variations associated with different MPPT behaviors of the inverter are also observed.

When the smart glass operates in the opaque mode, the electrical output of the PV module reaches its maximum level, while the transmission of solar radiation to the indoor environment decreases to a minimum. In this operating mode, the solar-based thermal energy entering the interior is reduced to negligible levels. When the smart glass switches to the transparent mode, a partial decrease in PV power generation is observed, whereas solar transmittance and the associated thermal gain reach their maximum level. The PV cells cover approximately 62% of the module surface, and the remaining 38%, consisting of the gaps between the cells, allows solar radiation to pass into the indoor space when the smart glass is in transparent mode. Since the amount of radiation transmitted directly through the PV cells themselves is very low, this effect is neglected.

An ANSYS finite element model representing the multilayer structure of the system is developed. In the model, the PV module, the air gap, and the PDLC layer are defined as separate layers, and the opaque and transparent modes of the PDLC are modeled using an effective irradiance approach. Table 2 summarizes the parameters used in the ANSYS model for each layer. Parameters that do not affect the results are neglected in this study such as the light transmittance of the air gap. Additionally, Figure 3 presents the ANSYS-based modeling of the system.

Table 2. Material properties.

	Density	Thermal Conductivity	Specific Heat	Absorptance	Transmittance	Reflectance
Glass1 & Glass2	2405 kg/m^3	0.98 W/m·°C	1250 J/kg·°C	0.045	0.951	0.004
EVA1 & EVA2	945 kg/m^3	0.35 W/m·°C	2090 J/kg·°C	0.02	0.95	0.03
Cell	2330 kg/m^3	148 W/m·°C	700 J/kg·°C	0.97	0	0.03
Air Gap	1.2 kg/m^3	0.026 W/m·°C	1005 J/kg·°C	0	1	0
Glass3 & Glass4	2405 kg/m^3	0.98 W/m·°C	1250 J/kg·°C	0.045	0.951	0.004
EVA3 & EVA4	945 kg/m^3	0.35 W/m·°C	2090 J/kg·°C	0.02	0.95	0.03
PDLC (Transparent)	960 kg/m^3	0.19 W/m·°C	1800 J/kg·°C	0.12	0.78	0.1
PDLC (Opaque)	960 kg/m^3	0.19 W/m·°C	1800 J/kg·°C	0.25	0.2	0.55

3. Test and Results

The experimental studies aim to analyze the electrical performance and thermal behavior of the system under different solar irradiance levels. Figure 4 presents images from the testing stages of the PV–smart glass module. The tests are conducted separately for the opaque and transparent operating modes of the smart glass. In addition, a reference PV module, identical in technical specifications but without smart glass integration, is included in the experimental process for comparison. All tests are carried out under identical environmental and operating conditions, and three different measurement results are obtained for each test scenario.

During the experiments, ambient temperature, PV module temperature, current and voltage at the maximum power point, maximum output power, solar irradiance incident on the module surface, and the amount of energy delivered to the grid are measured. The obtained experimental data are evaluated through comparison, and the results are summarized in Table 3. Gray rows indicate the transparent mode of the smart glass. Blue rows represent the opaque mode. Green rows show the results of the reference PV module without smart glass integration. When the opaque and transparent operating modes of the smart glass are compared, electricity generation is observed to be approximately 5% higher in the opaque mode. In addition, when the PV module without smart glass is compared with the PV module integrated with smart glass operating in opaque mode, the smart glass-integrated structure produces approximately 4% more electrical energy.

These results indicate that smart glass integration, when operated in an appropriate mode, can positively influence the overall electrical performance of the PV system. Furthermore, from a circuit-modeling perspective, the measured data in Table 3 can be used to obtain an approximate one-diode or two-diode representation of the PV-PDLC panel. The irradiance, ambient temperature, PV temperature, maximum power point current, maximum power point voltage, and DC power provide the main operating-point information required for parameter estimation. In a simplified one-diode model, the photocurrent can be approximated from the irradiance-dependent current, while the MPP values can be used as fitting points for estimating the diode saturation current, ideality factor, and series resistance. For a two-diode model, an additional recombination current branch may be included; however, accurate extraction of all parameters would require complete I-V curve measurements under different irradiance and temperature conditions.

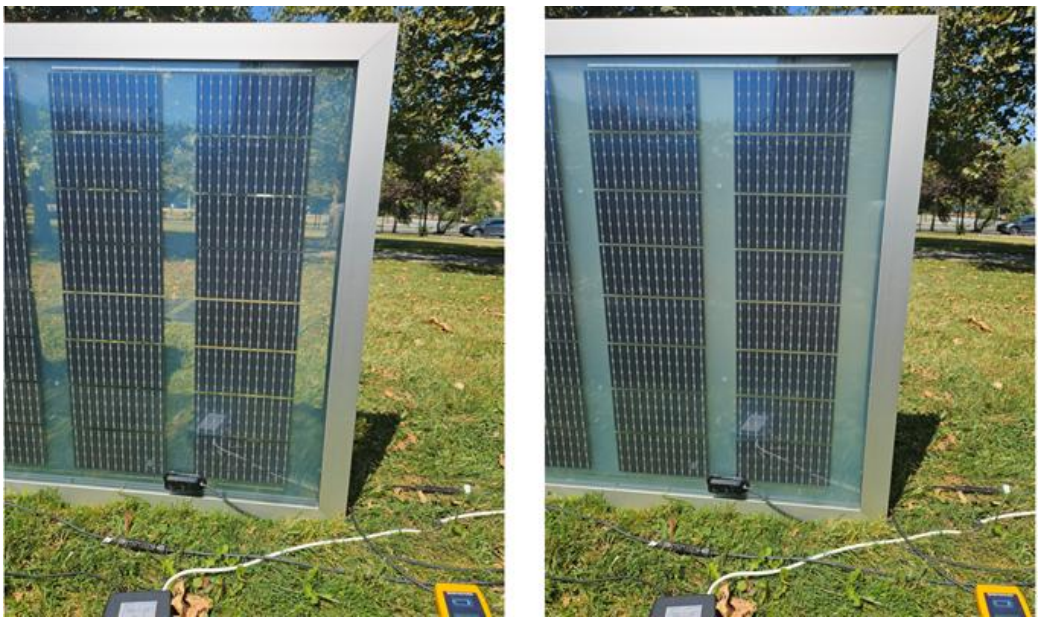


Figure 4. Transparent and opaque states in the testing phases of smart glass PV modules.

Table 3. Smart glass PV module test results.

Type	I_{AC}	V_{AC}	P_{AC}	*Irradiance*	I_{mppt}	V_{mppt}	P_{dc}	T_{amb}	T_{PV}	*"On" Mode Benefit*	
PV + Smart glass/Transparent	0.803 A	231.60 V	185.939 W	948 W/m^2	6.890 A	29.690 V	204.56 W	28.0 °C	40.0 °C	0.950	−5.0%
PV + Smart glass/Opaque	0.845 A	231.60 V	195.733 W	948 W/m^2	7.170 A	30.040 V	215.39 W	28.0 °C	43.0 °C	1.000	4–5%
PV	0.807 A	231.60 V	186.827 W	948 W/m^2	6.920 A	29.707 V	205.57 W	28.0 °C	39.0 °C	0.954	−4.6%
PV + Smart glass/Transparent	0.628 A	231.65 V	145.390 W	887 W/m^2	6.410 A	25.167 V	161.32 W	30.0 °C	54.0 °C	0.942	−5.8%
PV + Smart glass/Opaque	0.667 A	231.65 V	154.489 W	887 W/m^2	6.710 A	25.521 V	171.25 W	30.0 °C	61.0 °C	1.000	5.0%
PV	0.638 A	231.65 V	147.853 W	887 W/m^2	6.480 A	25.302 V	163.96 W	30.0 °C	52.0 °C	0.957	−4.3%
PV + Smart glass/Transparent	0.336 A	231.50 V	77.820 W	487 W/m^2	3.640 A	25.078 V	91.28 W	30.0 °C	55.0 °C	0.953	−4.7%
PV + Smart glass/Opaque	0.352 A	231.50 V	81.552 W	487 W/m^2	3.770 A	25.412 V	95.80 W	30.0 °C	61.0 °C	1.000	4.0%
PV	0.340 A	231.50 V	78.703 W	487 W/m^2	3.670 A	25.183 V	92.42 W	30.0 °C	52.0 °C	0.965	−3.5%
PV + Smart glass/Transparent	0.415 A	231.45 V	96.012 W	585 W/m^2	4.370 A	25.219 V	110.21 W	30.0 °C	56.0 °C	0.960	−4.0%
PV + Smart glass/Opaque	0.432 A	231.45 V	99.897 W	585 W/m^2	4.530 A	25.343 V	114.80 W	30.0 °C	60.0 °C	1.000	4.0%
PV	0.417 A	231.45 V	96.403 W	585 W/m^2	4.380 A	25.302 V	110.82 W	30.0 °C	54.0 °C	0.965	−3.5%
PV + Smart glass/Transparent	0.302 A	231.45 V	69.830 W	513 W/m^2	3.380 A	24.797 V	83.81 W	30.0 °C	55.0 °C	0.955	−4.5%
PV + Smart glass/Opaque	0.319 A	231.45 V	73.891 W	513 W/m^2	3.520 A	24.943 V	87.80 W	30.0 °C	58.0 °C	1.000	4.0%
PV	0.307 A	231.45 V	71.147 W	513 W/m^2	3.400 A	24.910 V	84.69 W	30.0 °C	52.0 °C	0.965	−3.5%
PV + Smart glass/Transparent	0.260 A	231.45 V	60.225 W	432 W/m^2	2.860 A	24.721 V	70.70 W	30.0 °C	53.0 °C	0.954	−4.6%
PV + Smart glass/Opaque	0.276 A	231.45 V	63.820 W	432 W/m^2	2.970 A	24.957 V	74.12 W	30.0 °C	56.0 °C	1.000	4.0%
PV	0.266 A	231.45 V	61.610 W	432 W/m^2	2.880 A	24.908 V	71.74 W	30.0 °C	51.0 °C	0.968	−3.2%

Furthermore, Figure 5 illustrates the DC power output of three different PV configurations as a function of solar irradiance ranging from 432 W/m^2 to 948 W/m^2. As

anticipated, a strong linear correlation is observed between solar irradiance and power generation across all systems. Notably, the PV + Smart glass (Opaque) configuration consistently outperforms both the standalone PV and the transparent counterpart across the entire irradiance spectrum, reaching a peak output of 215.39 W at 948 W/m^2. This performance enhancement can likely be attributed to the reduced light transmission in the opaque state, which increases photon absorption or optimizes thermal management within the integrated layer. Conversely, the PV + Smart glass (Transparent) integration exhibits a minor reduction in power output compared to the reference PV system, a trade-off primarily driven by the optical losses inherent to the transparent glass layer. These findings highlight the trade-offs between optical transparency and electrical efficiency in BIPV.

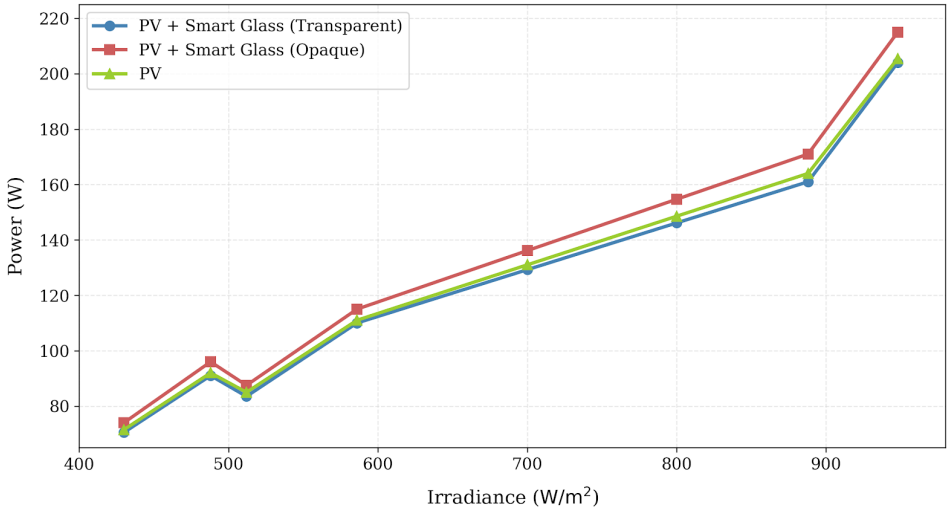


Figure 5. DC power output of three different PV configurations.

To quantitatively validate the ANSYS thermal model, the simulated PV surface temperatures are compared with the experimental temperature measurements for each panel configuration in Table 4. The coefficient of determination (R^2) and the root mean square error (RMSE) are used as validation indicators. For the PV–smart glass transparent mode, the calculated (R^2) and RMSE values are 0.82 and 2.35 °C, respectively. For the opaque mode, the corresponding values are 0.76 and 3.03 °C. For the reference PV module, the (R^2) and RMSE values are 0.594 and 3.19 °C, respectively. Considering all validation points together, the overall (R^2) and RMSE values are 0.783 and 2.88 °C. These results indicate that the ANSYS model represents the thermal behavior of the proposed PV–smart glass structure with acceptable accuracy. The relatively lower (R^2) value for the reference PV case is attributed to the limited number of experimental points and the narrow temperature variation range.

Table 4. Temperature values under different irradiance levels.

		948 W/m^2	**887 W/m^2**	**487 W/m^2**	**585 W/m^2**	**513 W/m^2**	**432 W/m^2**
Real	PV + Smart glass/Transparent	40 °C	54 °C	55 °C	56 °C	55 °C	53 °C
	PV + Smart glass/Opaque	43 °C	60 °C	61 °C	60 °C	58 °C	56 °C
	PV	39 °C	52 °C	52 °C	54 °C	52 °C	51 °C
		948 W/m^2	**887 W/m^2**	**487 W/m^2**	**585 W/m^2**	**513 W/m^2**	**432 W/m^2**
ANSYS	PV + Smart glass/Transparent	42 °C	55 °C	54 °C	53 °C	52 °C	50 °C
	PV + Smart glass/Opaque	44 °C	58 °C	57 °C	56 °C	55 °C	53 °C
	PV	41 °C	50.4 °C	49.5 °C	49 °C	48.5 °C	47.7 °C

During the tests, the thermal behavior of the PV module is continuously monitored using a thermal camera. According to the obtained results, when the smart glass operates in the opaque mode, the PV module temperature increases by approximately 7% compared to the transparent mode. Figure 6 presents a sample thermal image obtained from the thermal camera measurements. Figure 7a–c show the results of the ANSYS analysis of PV module, transparent mode of BIPV, and opaque mode of BIPV, respectively. Since each layer is separately defined in the ANSYS model and the material properties are introduced in detail, the theoretical results show good agreement with the experimental findings.

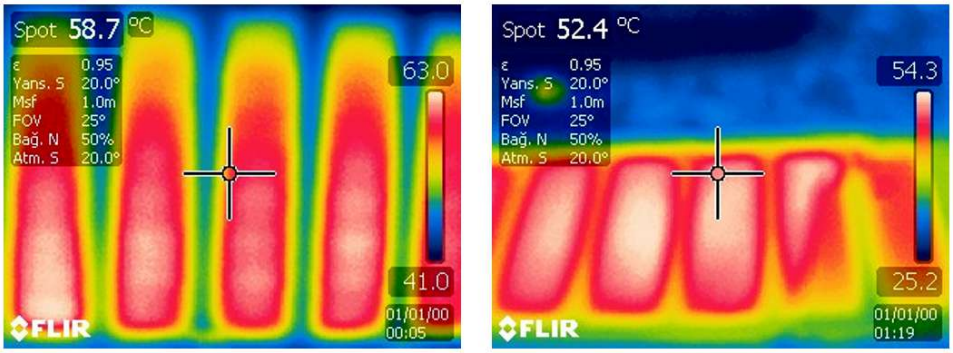


Figure 6. Thermal camera measurement of the smart glass–integrated PV module.

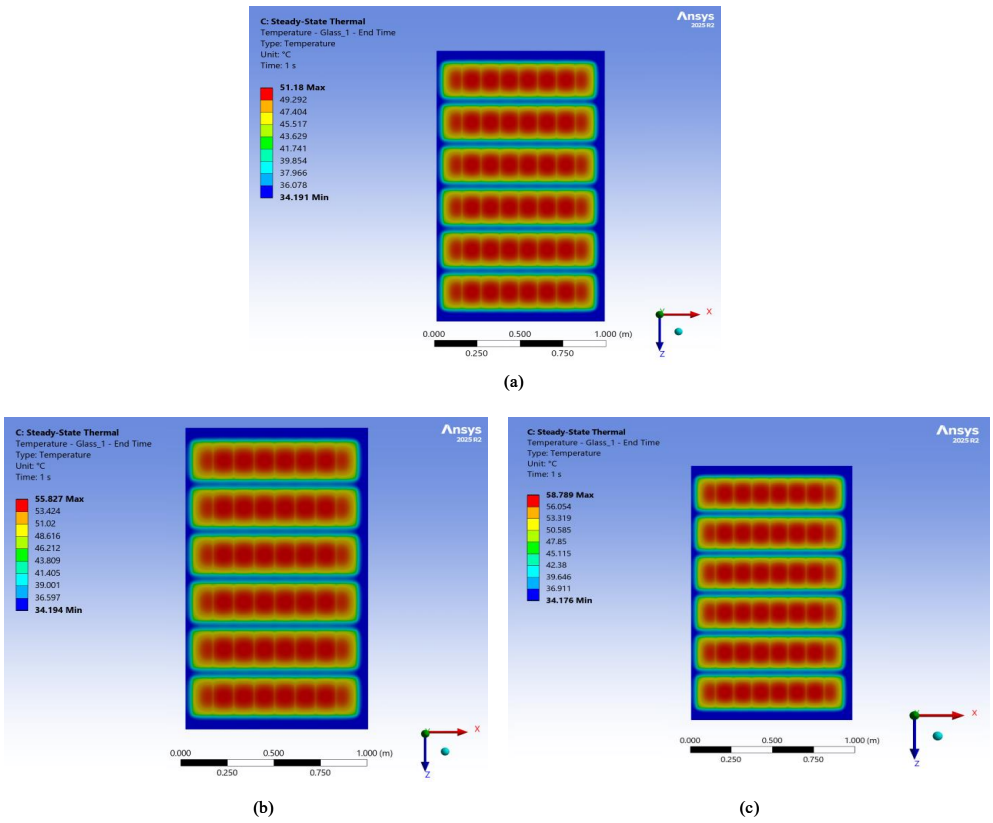


Figure 7. (**a**) ANSYS analysis of PV module, (**b**) ANSYS analysis of transparent mode of BIPV, (**c**) ANSYS analysis of opaque mode of BIPV.

When low and high irradiance levels are compared at similar module temperatures, the difference between the opaque and transparent modes becomes clearer. The opaque mode provides a more pronounced increase in electricity generation under high irradiance conditions. This indicates that, at increased irradiance levels, the opaque mode enhances the effective irradiance on the PV cells, making power generation at the maximum power

point more advantageous. The results demonstrate that the operating mode of the smart glass is a critical parameter that directly influences not only indoor comfort but also the electrical performance of the PV module.

4. Discussion

The uncertainty of the experimental results is mainly associated with the measurement accuracy of the irradiance sensor, electrical measurement units, and thermal camera. Since the tests were performed under real outdoor conditions, variations in solar irradiance and ambient temperature may also contribute to the uncertainty of the measured power and temperature values. However, all configurations were tested under identical environmental and operating conditions, and the results were evaluated comparatively. Therefore, the relative differences between the transparent mode, opaque mode, and reference PV module provide a reliable indication of the performance trend of the proposed system.

On the other hand, although the proposed system shows promising electrical and thermal performance, this study has some limitations. The experimental tests were conducted under real outdoor conditions but at discrete irradiance levels. Therefore, long-term seasonal performance, daily operating stability, and degradation effects were not evaluated. The analysis was also limited to a prototype-scale PV–smart glass module. In addition, the thermal model was developed using selected material properties and simplified boundary conditions. Economic feasibility, life-cycle performance, and large-scale façade integration were not considered in this study. These issues should be investigated in future studies to better evaluate the practical applicability of the proposed system.

It should also be noted that this study focuses on the electrical output and module-level thermal behavior of the proposed PV–smart glass system. Indoor building-performance indicators were not directly measured. Parameters such as indoor illuminance, glare index, solar heat gain, room thermal load, and occupant comfort were outside the scope of the present experimental study. Therefore, the indoor comfort-related discussion should be interpreted as a potential benefit of the controllable optical behavior of the PDLC layer, not as a directly validated indoor performance result. Future studies should include room-scale experiments or building energy simulations to evaluate daylight availability, glare risk, indoor thermal load, and occupant comfort in detail.

5. Conclusions

In this study, a novel BIPV technology based on the integration of smart glass and a PV module was proposed, combining energy generation and user comfort within a single building component. The system was based on the integration of a 240 Wp PV panel and an electrically controllable laminated smart glass into one module. This structure enabled both electricity generation and the dynamic management of indoor lighting and thermal comfort.

Thanks to its adjustable transparency, the smart glass not only improved user comfort but also supported PV performance by contributing to the redirection of radiation that did not directly reach the cells. Experimental results showed that the integrated system generated approximately 4% more energy than a conventional PV application, and that electricity production in opaque mode was about 5% higher than in transparent mode.

From a manufacturing perspective, the main additional complexity of the proposed PV-PDLC panel is related to the integration of the PDLC glazing layer, electrical connections, air gap control, and multilayer frame assembly. The overall cost is expected to be mainly affected by the PDLC glass area, lamination quality, control electronics, and installation requirements. In future studies, long-term performance analysis of the proposed system under different climatic conditions, its scalability, and the optimization of manu-

facturing processes can be investigated. In addition, further development of the system architecture through alternative design variations and a more detailed evaluation of the cost–performance balance will enhance the commercialization potential of the technology.

Author Contributions: Methodology, T.B.; writing—original draft preparation, T.B.; writing—review and editing, T.G., A.R.B. and İ.K.; visualization, T.G.; supervision, A.R.B. and İ.K. All authors have read and agreed to the published version of the manuscript.

Funding: This study was funded by the Scientific Research Projects Coordination Unit of Yildiz Technical University under Project No. FBA-2022-4997.

Data Availability Statement: The original contributions presented in this study are included in the article. Further inquiries can be directed to the corresponding author.

Conflicts of Interest: Author T.B. was employed by Dal Solar Energy during the conduction of this study. All authors declare that the research was conducted in the absence of any commercial or financial relationships that could be construed as potential conflicts of interest.

References

1. Chen, X.; Xie, Q.; Cao, X. Do climate mitigation policies reduce within-country carbon inequality? Evidence from cross-national panel data. *Energy Policy* **2026**, *210*, 115056. [CrossRef]
2. Yue, Z.; Fu, X. Green actions in policy fog: Climate policy uncertainty and corporate carbon emission. *Int. Rev. Econ. Financ.* **2026**, *105*, 104802. [CrossRef]
3. Bibih, M.; Choukri, K.; El-Khaili, M.; Chakir, H. Enhancing Grid Flexibility and Facilitating Renewable Energy Integration through the Evaluation of Green Hydrogen's Role. *IFAC-PapersOnLine* **2024**, *58*, 258–265. [CrossRef]
4. Wu, Y.; Huang, H.; Cao, Y.; Wang, B.; Li, X.; Song, X.; Pang, Z.; Jiang, T.; Lu, Y.; Tan, G. Photovoltaic material selection and multi-objective building design optimization for enhancing energy performance of building integrated photovoltaics (BIPV) systems. *Appl. Energy* **2026**, *406*, 127270. [CrossRef]
5. Aleem, A.; Habib, U.; Salman, W.; Saeed, M.T. Designing glass materials for renewable-energy production through building integrated photovoltaics (BIPV)—A computational approach. *Energy Build.* **2026**, *356*, 117108. [CrossRef]
6. Xie, Y.; You, T.; Dai, B.; Cui, H. A review of colored building-integrated photovoltaics (BIPV) for building decarbonization: Technological and market perspectives. *Renew. Sustain. Energy Rev.* **2026**, *235*, 116924. [CrossRef]
7. Aguacil, S.; Duque, S.; Lufkin, S.; Rey, E. Designing with building-integrated photovoltaics (BIPV): A pathway to decarbonize residential buildings. *J. Build. Eng.* **2024**, *96*, 110486. [CrossRef]
8. Ghosh, A. Thermal-optical-electrical performance of combined photovoltaic-polymer dispersed liquid crystal for switchable BIPV-smart window. *J. Build. Eng.* **2026**, *121*, 115655. [CrossRef]
9. Chen, L.; Baghoolizadeh, M.; Basem, A.; Ali, S.H.; Ruhani, B.; Sultan, A.J.; Salahshour, S.; Alizadeh, A. A comprehensive review of a building-integrated photovoltaic system (BIPV). *Int. Commun. Heat Mass Transf.* **2024**, *159*, 108056. [CrossRef]
10. Dias, J.B.; da Graça, G.C. Using building thermal mass energy storage to offset temporary BIPV output reductions due to passing clouds in an office building. *Build. Environ.* **2022**, *207*, 108504. [CrossRef]
11. Rajoria, C.S.; Kumar, R.; Sharma, A.; Singh, D.; Suhag, S. Development of flat-plate building integrated photovoltaic/thermal (BIPV/T) system: A review. *Mater. Today Proc.* **2021**, *46*, 5342–5352. [CrossRef]
12. Hendinata, L.K.; Fikri, A.I.R.; Suprapto, M.A. Design of Integrated Electrochromic-Photovoltaic Technology for Smart Windows to Improve Building Performance and Energy Efficiency: A Material Approach. *Indones. J. Energy* **2022**, *5*, 1–14. [CrossRef]
13. Cánovas-Saura, A.; Ruiz, R.; López-Vicente, R.; Abad, J.; Urbina, A.; Padilla, J. Portable Photovoltaic-Self-Powered Flexible Electrochromic Windows for Adaptive Envelopes. *Electron. Mater.* **2021**, *2*, 174–185. [CrossRef]
14. Huang, L.-M.; Hu, C.-W.; Liu, H.-C.; Hsu, C.-Y.; Chen, C.-H.; Ho, K.-C. Photovoltaic electrochromic device for solar cell module and self-powered smart glass applications. *Sol. Energy Mater. Sol. Cells* **2012**, *99*, 154–159. [CrossRef]
15. Ma, R.-H.; Chen, Y.-C. BIPV-Powered Smart Windows Utilizing Photovoltaic and Electrochromic Devices. *Sensors* **2012**, *12*, 359–372. [CrossRef] [PubMed]
16. Xie, Y.; Li, M.; Liu, J.; Cao, N.; Gu, G.; Chao, D. Photovoltaic-driven electrochromic smart windows for net-zero energy buildings. *Chem. Eng. J.* **2025**, *524*, 169847. [CrossRef]
17. Zhang, W.; Wu, X.; Xie, L.; Zhao, O.; Zhong, J.; Zeng, X.; Zou, R. Study on the impact of photovoltaic electrochromic modular smart window on indoor environment. *Build. Environ.* **2023**, *238*, 110381. [CrossRef]
18. Tan, Y.; Peng, J.; Luo, Z.; Luo, Y.; Li, H. Assessing the energy efficiency and grid friendliness of smart photovoltaic windows incorporating crystalline silicon cells and electrochromic film. *Appl. Energy* **2025**, *377*, 124671. [CrossRef]

19. Wu, X.; Zhang, W.; Xie, L.; Zhao, O.; Chen, M.; Li, Z.; Li, J. Study on the Performance of Photovoltaic Electrochromic Window System and Impact on Indoor Lighting Environment. In Proceedings of the Applied Energy Symposium 2020: Low Carbon Cities and Urban Energy Systems, Virtually, 10–17 October 2020. [CrossRef]
20. Wu, X.; Zhang, W.; Xie, L.; Zhao, O.; Li, Z.; Li, J.; Zhong, J. Study on the impact of partition photovoltaic electrochromic windows on building lighting environment and energy saving. *Energy Build.* **2023**, *280*, 112722. [CrossRef]
21. Martín-Chivelet, N.; Guillén, C.; Trigo, J.F.; Herrero, J.; Pérez, J.J.; Chenlo, F. Comparative Performance of Semi-Transparent PV Modules and Electrochromic Windows for Improving Energy Efficiency in Buildings. *Energies* **2018**, *11*, 1526. [CrossRef]
22. Zheng, Y.; Miao, J.; Yu, H.; Liu, F.; Cai, Q. Thermal Analysis of Air-Cooled Channels of Different Sizes in Naturally Ventilated Photovoltaic Wall Panels. *Buildings* **2023**, *13*, 3002. [CrossRef]

Disclaimer/Publisher's Note: The statements, opinions and data contained in all publications are solely those of the individual author(s) and contributor(s) and not of MDPI and/or the editor(s). MDPI and/or the editor(s) disclaim responsibility for any injury to people or property resulting from any ideas, methods, instructions or products referred to in the content.